High Energy Physics and Nuclear Physics

Volume 16, Number 4

Study of Radiation Damage of a Tile/Fiber Scintillator Calorimeter

Mao Huishun,[1] Wang Guoliang,[1] Liu Nianzong,[1] Zhang Ge,[1] Zhang Zhuxiang,[1] Zhang Liangsheng,[1] Zhang Caidi,[1] Zheng Linsheng,[1] Zhou Yongshen,[1] Hu Lidong,[1] Zhao Xiaojian,[1] Zhong Xuechu,[1] Tan Yiping,[1] Han Shiwen,[1] D. Green,[2] A. Para,[2] and K. Johnson[3]

[1](Institute of High Energy Physics, CAS, Beijing, China)
[2](Fermilab, USA)
[3](Florida State University, USA)

The measurements of radiation damage of a tile/fiber scintillator modules to be used for the SDC calorimeter are described. Four tile scintillator modules were irradiated up to 6 Mrad with the BEPC 1.1 GeV electron beam. We have studied the light output at different depths in the modules and for different integrated doses. The recovery process and the dependence of radiation damage on the ambient atmosphere are also investigated.

1. INTRODUCTION

The solenoidal detector collaboration (SDC) is a large general spectrometer, which has been the only (thus far) approved detector at the super superconducting collider (SSC). The SDC calorimeter, an important part of the SDC, has been planned on the technology of interspersed scintillator and Pb (or Fe) absorber plates with wavelength shifting fibers used to transport the light to the rear for photomultiplier tube (PMT) readout. Some SDC tracking technology also requires use of plastic scintillators. The plastic scintillator has many advantages (e.g., fast response, simple readout, suitability for work at very high luminosity, simple structure, and ease of construction and operation). It is absolutely critical to establish that plastic scintillators will withstand certain radiation doses, especially that set as the integrated dose for 10 years of SSC running at a luminosity of $10^{34}/cm^2 \cdot s$. Without such tests, plastic scintillators cannot be considered as a viable candidate technology for either tracking or calorimetry.

Received on September 28, 1991.

The radiation at the SSC in p-p collisions is mostly due to the produced charged and neutral particles. Since all the energy of an electromagnetic shower is deposited in a region of limited depth, most of the effects of radiation damage on the calorimeter performance are due to the production of electromagnetic showers in the calorimeter itself, through the 2γ decay of π°. These photos will have energies typically in the range of a few GeV. This allows us to use an electron beam of about 1 GeV as an optimum source for the study of radiation damage in the multi-TeV SSC operational environment. We adopted the BEPC (Beijing electron positron collider) electron beam at 1.1 GeV as the radiation source for radiation damage tests. Four tile/fiber scintillator modules were irradiated stepwise up to 6 Mrad. We studied their light output at different depths in the modules and at different integrated doses. The recovery process and the dependence of radiation damage on the ambient environment, nitrogen, and air, is also studied.

2. SCINTILLATOR TILE CALORIMETER MODULE

Figure 1 shows the structure of the scintillator tile module. A standard tile module consists of 21 Pb plates of absorber, interspaced with 20 scintillator tiles. The scintillating tile is a polystyrene-based scintillator, SCSN81, and is 2.5 mm thick. The Pb plate is 5 mm thick. The area of each tile is about 11 cm × 11 cm, and the Pb plate is 12.7 cm × 12.7 cm. The light output from the scintillator is collected using BCF91 (Bicron Co.) wavelength shifter fibers, which were directly connected to a photomultiplier tube (such as XP 2020) with no depth segmentation.

The fiber (BCF91) consists of a central core of doped polystyrene (PS), with a diameter of 1 mm, surrounded by a lower refractive index cladding (PMMA) of several micron thickness. The fibers are embedded in the scintillating plastic tiles without glue and connected tightly to the PMT without silicon oil to prevent radiation damage from glue and silicon oil.

All of the Pb plates, tiles, and fibers (except the PMT) are in an Al box.

3. TEST BEAM AND DOSAGE MONITORING

The radiation source is e^- test beam of BEPC. The typical characteristics of the beam include: 600-mA peak current, 2.5-ns pulse duration at 12.5 Hz, 1-cm^2 beam spot size, and about 1.1×10^{11} $e^-/cm^2 \cdot s$ which is equivalent to an average current of about 18.75 nA/cm^2.

The beam position and spot size can be monitored in the control room by three fluorescent screens, and can be controlled with a set of magnets in beam line. We also put a fluorescent screen on the front surfaces of modules to monitor the beam position and spot size.

A beam current transformer (BCT) was put at the end of the beam line to monitor both intensity and integrated dose available during irradiation. The area of the BCT pulse is accurately proportional to the electron flux (in number of electrons). The BCT pulses were sent to an ADC and gated by the BCT pulse. An IBM/PC computer acquired the ADC data through CAMAC system and converted them into intensity and integrated dosage. The BCT and ADC both were precalibrated by an accurate pulse generator first, and then calibrated by the beam. The conversion from incident electron flux to dosage in rad at shower maximum is calculated to be, 1 rad $= 3 \times 10^6$ e^-/cm^2. The calculation takes in account the structure of module and the energy of electron beam.

In order to obtain accurate dosimetry, the radiochromic films were incorporated in the test modules, 5 pieces of film at shower maximum and 5 other pieces on the front face of every test module. By measuring the transmission before and after irradiation for a certain wavelength with a monochrometer, the approximate dose can be calculated [1] and will be used to check the BCT value.

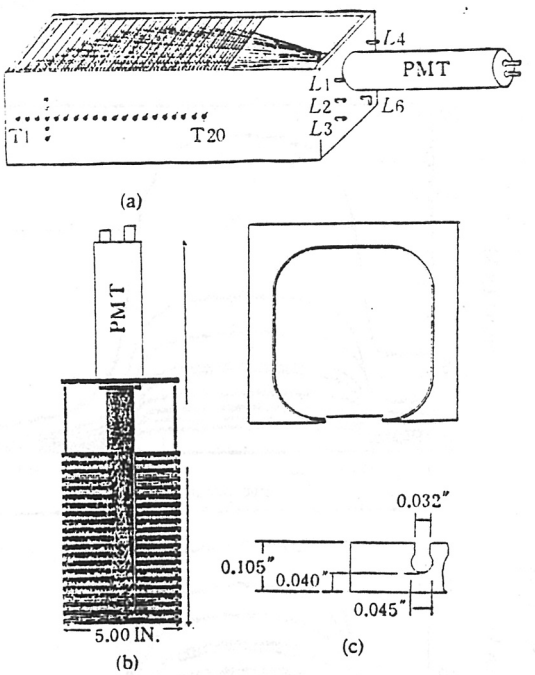

Fig. 1
Scintillating tile/fiber calorimeter module.
(a) Sketch; (b) Photo; (c) Typical tile/fiber coupling.

4. EXPERIMENTAL APPARATUS AND PROCEDURE

4.1 Module's Arrangement and Movable Table

Four tested modules, called tile modules #1, #2, #5, and #6 were mounted on a movable table. The modules and the table have a common support, which can be moved. The table is motorized and capable of moving both horizontally (x) and vertically (z) by remote control. Railway track was laid on the floor in the test beam area to move the common support in or out. During irradiation, the table was moved in both x and z directions continuously in order to achieve uniform irradiation. The moving speed of the table is ~30 mm/s in the x direction and only 0.75 mm/s in the z direction.

4.2 Source Driver and Calibration [2]

A moving radioactive source was used to calibrate and measure the performance of the tile/fiber calorimeter module before and after irradiation. The source is ^{137}Cs, 6.8 mCi, 0.71 mm in diameter, 1.1 cm in length and is fixed to the front end of a fine metal wire, which is 6 m long and 0.71 mm in diameter. The design [2] of the source driver has a remotely actuated driver capable of pushing a fine metal wire carrying a radioactive source through any one of a large number of fine plastic and metal tubes into various parts of a calorimeter.

Each module has 24 transverse tubes (T1, T2, ···, T20 and 2 tubes above and 2 tubes below T4) starting from the side of the modules, each module also having 6 longitudinal tubes (L1, L2, ···, L6) starting from the back of the module and crossing the edge of all 20 scintillator-Pb plates (Fig. 1).

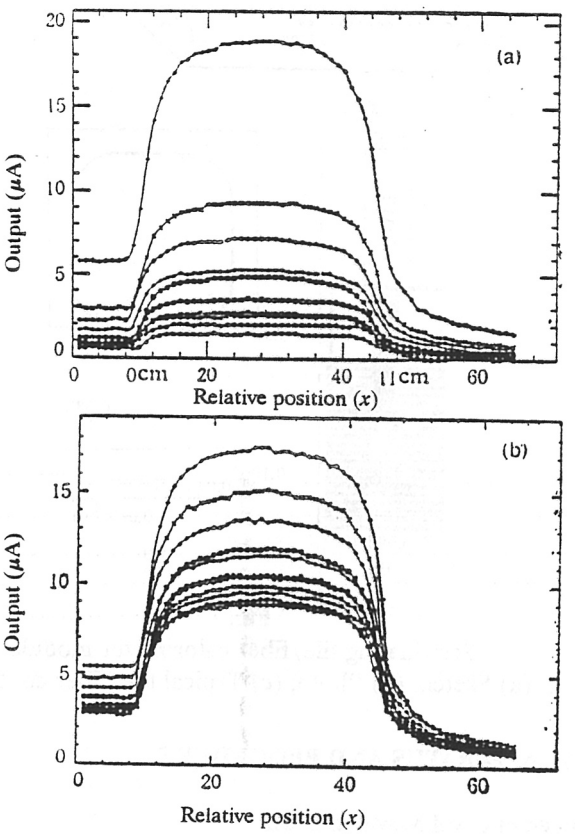

Fig. 2

Outputs at various positions (x) across the tiles of module #5 in air. (a) Tile #2; (b) Tile #18. The integrated doses, corresponding to the curves from top to bottom are 0.000, 0.300, 0.750, 1.125, 1.500, 2.250, 3.000, 3.750, 4.500, 5.250, 6.000 Mrad.

Before irradiation or after each irradiation step, the source was pushed into the profile of the module at high speed. We then measured the light output as the source was moving away from the module at slow speed. The damage to the profile of module can be determined from the light output.

4.3 Gas Environment

Tile modules #1 and #2 were kept in nitrogen during irradiation. After irradiating up to 6 Mrad, module #1 was still kept in N_2, but we let air into module #2 to observe its recovery process in an air atmosphere. Modules #5 and #6 were irradiated and annealed in the air.

4.4 Irradiation and Data Acquisition

The irradiating steps were 0.3, 0.45, 0.375, 0.375 Mrad, and then 0.75 Mrad stepwise up to a total of a 6-Mrad integrated dose. It is important to emphasize that module #6 was irradiated to 7.5 Mrad before this test. Therefore, module #6 has been irradiated up to a total of 13.5 Mrad.

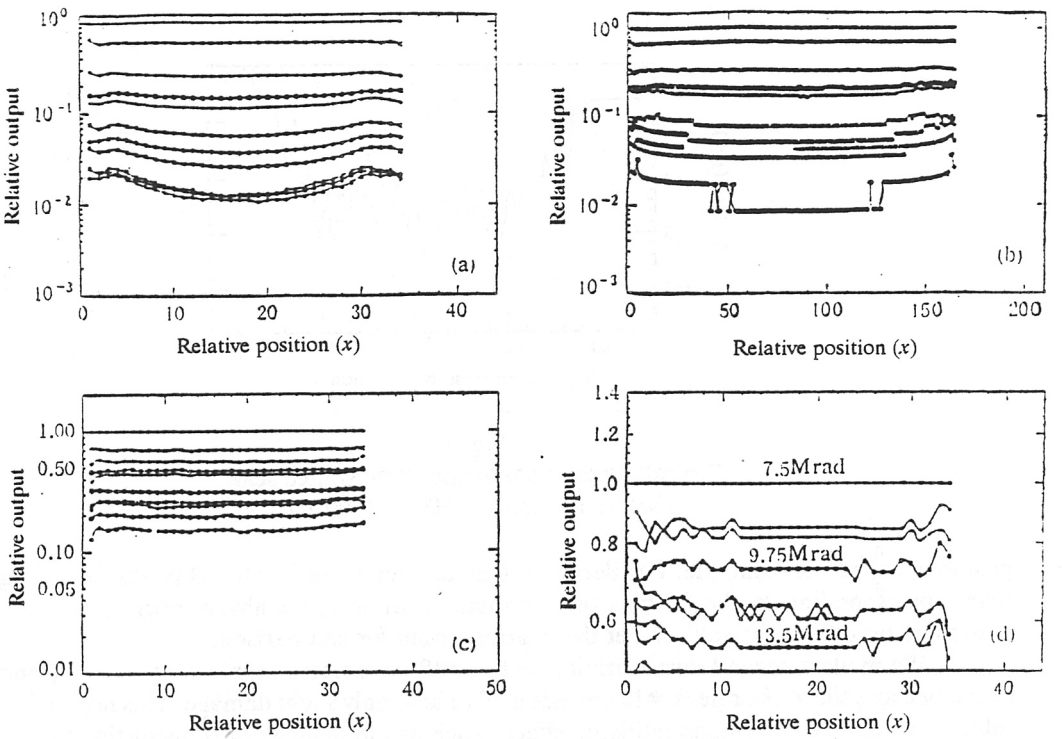

Fig. 3

Relative outputs (normalized to pre-irradiation) at various positions (x) across tile #6. (a), (b), (c), (d) are modules #1 and #2 in N_2, #5 and #6 in air, respectively. In (a), (c), the doses from top to bottom: 0.000, 0.300, 0.750, 1.125, 1.500, 2.250, 3.000, 3.750, 4.500, 5.250, 6.000 Mrad. In (b), the doses: 0.000, 0.300, 0.750, 1.125, 1.500, 2.250, 3.000, 3.750, 4.500 Mrad.

After every irradiating step, the PMT current from various profile of modules was measured as the source being pulled out from modules. The current was converted into voltage on the output resistor. The voltage was read-out by IBM/PC and CAMAC systems via a DSP2032 autoranging scanning DVM. These data, registered at definite time, corresponded to the light outputs at definite positions of modules.

The dark current (background) was also measured and registered with the DSP2023 readout system when the source was in the garage (Pb shielding box).

5. DATA ANALYSES AND RESULTS

5.1 Explanation of Data Analyses

1. It is very important to subtract the background current from the data before further analyses because irradiation activated the scintillator, and also the different operating status of accelerator caused the test area of the modules to have different radioactive environments.

2. To normalize the data to the pre-irradiation measurement, we took source data from every transverse and longitudinal tube for all four modules before irradiation and defined it as 0 Mrad data. We found that the outputs change for different tiles of the same module as well as for different

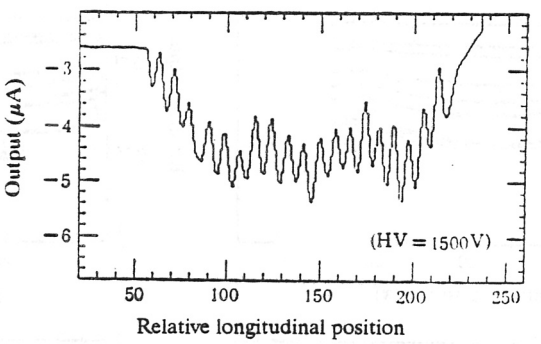

Fig. 4
Typical output from longitudinal source scan
(before irradiating, HV = 1500 V).

positions (x) of the same tile. Furthermore, they are not same for the 20 peaks for a longitudinal scan, corresponding to the 20 tiles of a module. Therefore, we always normalized the data to pre-irradiation data (0 Mrad), to get the relative output for comparison.

3. We made a second normalization to tile #18 (transverse scan) or peak #19 (longitudinal scan), because tile #18 or peak #19 are assumed to have only slight damage. This normalization can subtract or cancel some nonscintillator effects, such as the damage of transporting fibers and the coupling variation between fiber and PMT, due to the module's continuous movement during irradiation. The relative output, after second normalization, will mainly correspond to the damage of scintillator tile/fiber. Tile #18 was the last tile tested, which is why we only normalized to tile #18 for transverse scan. For peak #20, having a big edge effect, we only normalized the data to peak #19 for longitudinal scan.

5.2 Results

1) Transverse scan of source

Because of the different bending of the source tubes and different resistance in source tubes, the source speed varies. This causes the width of the output "broad peak" of the transverse profile to vary. Figure 2 shows a typical plot after correcting the peak width of the outputs at various positions (x) across a tile for different doses and is a good example because every tile of every module had a plot of this kind. From Fig. 2, we found that there were almost no current outputs at tile #2 near the shower maximum for integrated dose of 6 Mrad.

To get a clearer picture of the transverse nonuniformity of response caused by radiation damage, we plotted the ratio (normalized to pre-irradiation) of the response at various positions (x) across the tile at different doses. Figure 3 shows these plots at tile #6 of four modules. From these plots, we found that the transverse uniformity of response was quite good, especially for the lower doses ($\leq$1 Mrad). We observed scarcely any nonuniformity of the relative output either for module #1 or #2 under N_2 or for module #5 in air. The uniformity of module #6 is worse because it was irradiated from 7.5 Mrad to 13.5 Mrad.

2) Longitudinal scan of source (L2, L5)

Figure 4 is a typical output from longitudinal scan of source before irradiating, as a function of the depth in the module. The 20 peaks correspond to the 20 scintillator tiles. The form of the curves will change when the irradiating dose increases. There were almost no peaks at the tiles near shower maximum after irradiating up to high integrated doses. Figure 5 shows the longitudinal (depth)

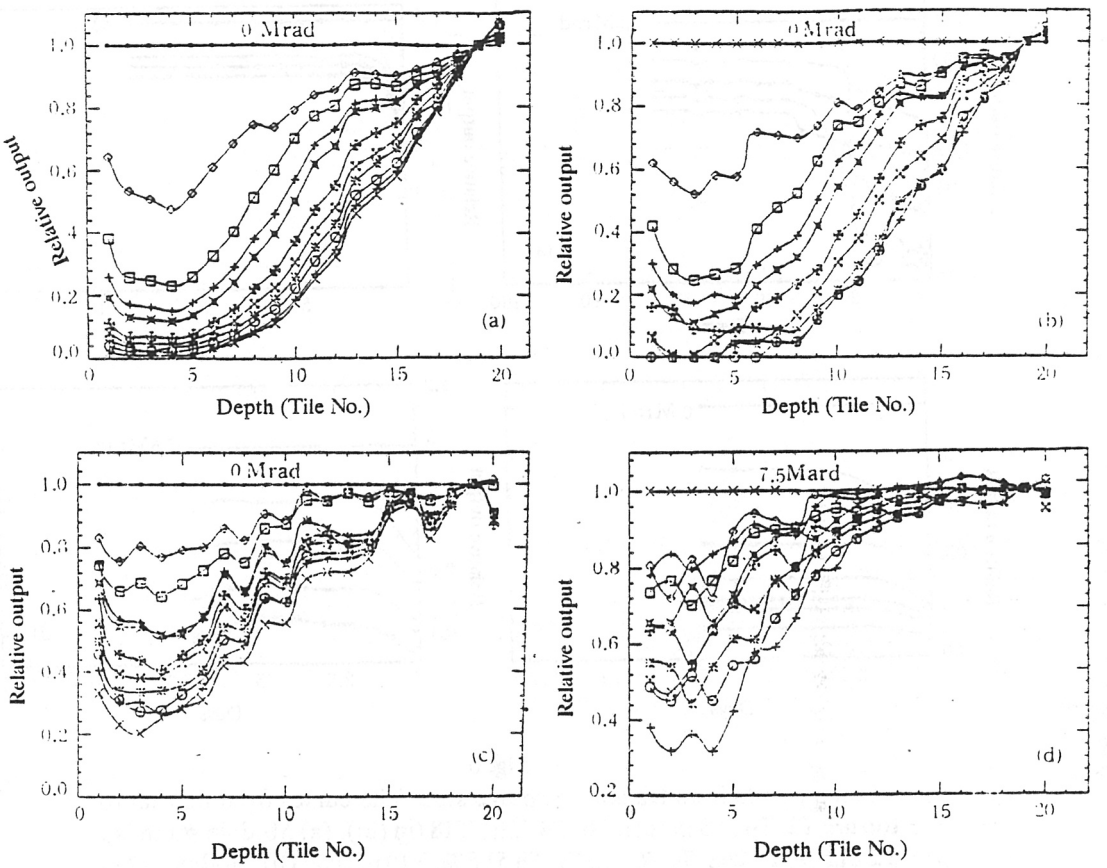

Fig. 5

Depth profile of damage from L2 source scan (normalized to peak #19) at various doses: 0.30, 0.75, 1.13, 1.50, 2.25, 3.00, 3.75, 4.50, 5.25, 6.00 Mrad. (a) Module #1 in N_2; (b) Module #2 in N_2; (c) Module #5 in air; (d) Module #6 in air.

◇ 0.30 Mrad, □ 0.75 Mrad, ✣ 1.13 Mrad, ⌘ 1.50 Mrad, ⊞ 2.25 Mrad, ⊠ 3.00 Mrad, ✳ 3.75 Mrad, ○ 4.50 Mrad, + 5.250 Mrad, × 6.00 Mrad.

profile of damage. The relative outputs in Fig. 5 were the values after two normalizations, normalized to pre-irradiating first, and then to peak #19 (the integrated dose for module #6 was still from 7.5 Mrad to 13.5 Mrad). These plots give us an effective damage profile as a function of the depth in the calorimeter at different doses, which coincided with the longitudinal development of an electromagnetic shower of a 1.1 GeV electron. The relative outputs of module #5 in air were larger than modules #1 and #2 in nitrogen at same doses.

3) Recovery after irradiation

There are two kinds of radiation damage [3], one permanent and the other, which can be annealed. In order to observe the recovery process, we continued to take data by scanning the source after irradiation stopped (integrated dose up to 6 Mrad). Figure 6 shows the recovery curves which are the relative outputs at center of tiles, normalized to pre-irradiating, as a function of times. Figure 7 is the relative output at different depth and different days, those data being measured from the

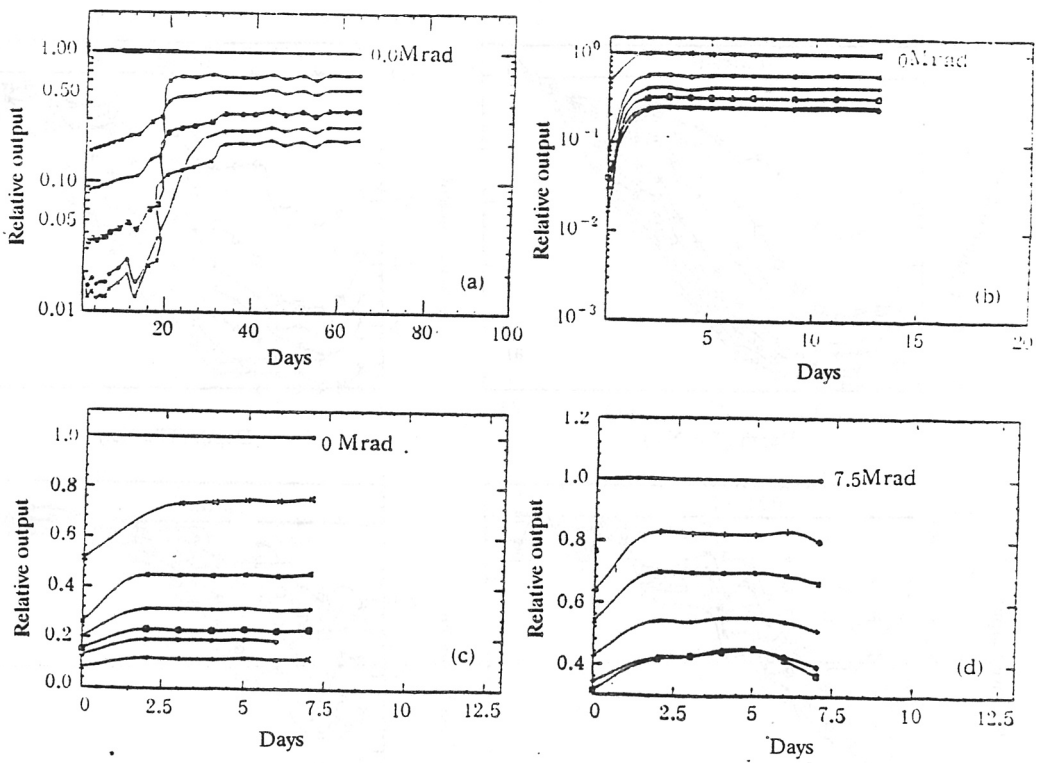

Fig. 6

Recovery plots from transverse source scan. The curves from bottom to top are T2, T4 (T5 in (c)), T6, T8, T10, T18 (in (c)). (a) Module #1 in N_2, T2 21.5%, T4 26.9%, T6 35.8%, T8 51.8%, T10 67.7%; (b) Module #2 in air; (c) Module #5 in air; (d) Module #6 in air.

longitudinal source scan and normalized to both pre-irradiating and peak #19. The outputs of pre-irradiating and after 6 Mrad radiation are also shown in Fig. 7 for clear comparison.

From Figs. 6 and 7, we see that the annealing rate depends very much on the gas condition. The recovery process of modules #2, #5, and #6, which were in the air, was largely completed in only two days, enabling the outputs to achieve a short term plateau. The recovery process of module #1, which was always kept in N_2 when irradiating or annealing, was much slower and continued to change until about 50 days (Figs. 6(a) and 7(a)).

The relative outputs of modules #1, #2, and #5 at damage maximum after recovery, were 28%, 26%, and 22%, respectively (Fig. 7). The recovered relative outputs of modules #1 and #2, irradiated in N_2, is a little larger than module #5 in air, indicating that the permanent radiation damage in N_2 is slightly smaller. However, the difference is so small that we can consider all of modules #1, #2, and #5 as having the same recovered relative output, about 25%. The facts that recovery in air is much faster than in N_2 and that their recovered relative outputs are almost the same explains why the output of module #5 in air is larger than modules #1 and #2 in N_2 during irradiation. This does not mean that the damage in air is smaller than in N_2 - rather, it shows that module #5 recovered faster during irradiation.

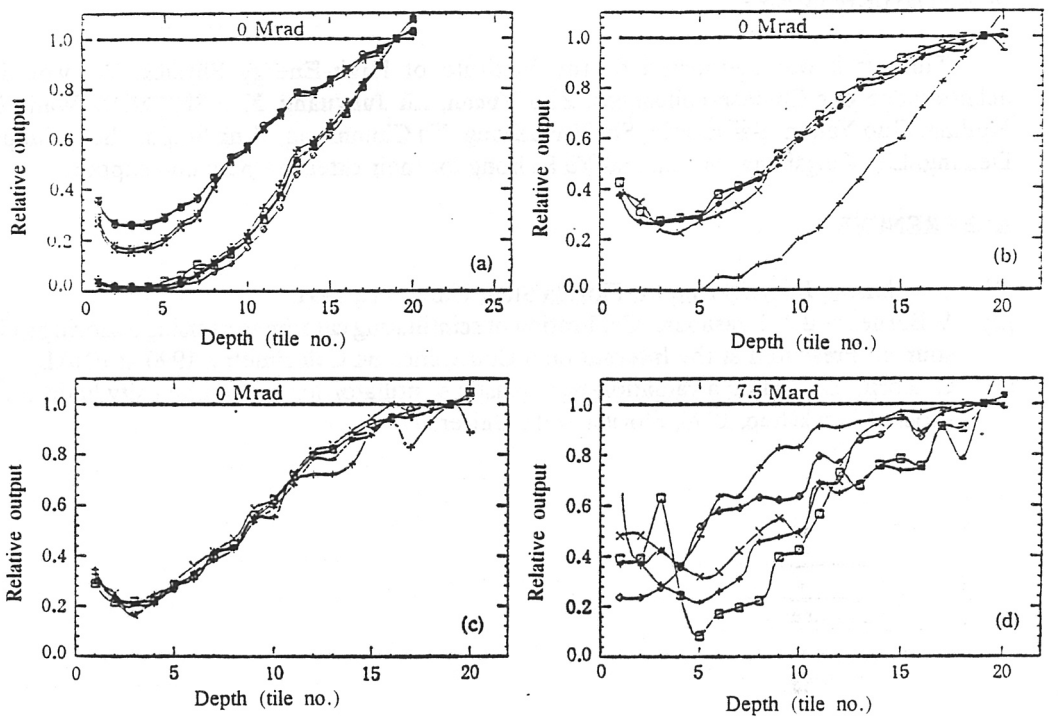

Fig. 7

Recovery Plots from Longitudinal Source Scan (L2).
(a) Module #1 in N_2, ◇ 6.0 Mrad 0 day, ▫ 2 days, ◇ 4 days, ⌑ 6 days, ⌖ 13 days, ⌘ 20 days, ⌖ 30 days, ○ 40 days, + 51 days, × 64 days; (b) Module #2 irradiating in N_2 and recovery in air; (c) Module #5 in air; (d) Module #6 in air. In (b), (c), (d): + 6 Mrad (or 13.5 for #6) 0 day, × 2 days, ◇ 3 days, ▫ 13 days, + 30 days.

6. CONCLUSIONS

1) The scintillating tiles near shower maximum are damaged to a large degree after irradiating up to 6 Mrad. After short term recovery, the output at shower maximum is reduced to about 25% of the initial output.

2) The fact the output of module #1 after recovery is a little larger than module #5 shows the permanent radiation damage in N_2 to be slightly smaller than in air. However, recovery in air is much faster than in N_2.

3) There also appeared a little recovery in module #6, when the output was normalized to the output at 7.5 Mrad. But the absolute outputs were really very small, even after recovery.

4) It is important that, based on our radiation damage data, the tile/fiber technique can be used in the SDC barrel calorimeter (0.6 Mrad total dose for 10 years at SSC design luminosity).

5) We used a commercial scintillator and PMT in this test. We will try other scintillating materials for tile/fiber and try another PMT with a different sensitive wavelength region. We want to find better material for radiation hardiness and less damage wavelength region. This will make the tile/fiber technique not only suitable for the barrel calorimeter but also a good candidate for end-cup calorimeter.

ACKNOWLEDGMENT

This work was supported by the Institute of High-Energy Physics. We would like to acknowledge our Chinese colleagues, Zhu Yucan, Lü Junguang, Xue Shengtian, Wang Man, Ni Huiling, Guo Yanan, Bai Jingzhi, Shi Huanzhang, Yu Chuansong, Tang Suqiu, Sheng Junpeng, Liu Dekang, Liu Yongsheng, Ma Li, and Ye Kairong for their extensive help and support.

REFERENCES

[1] K. Johnson, Internal Report, Florida State University, 1991.
[2] V. Barnes and A. Laasanen, "Calibration of scintillating calorimeters using a moving radioactive source," Presented at the International Conference on Calorimetry, 1990 at FNAL.
[3] C. Zorn, "Designing a radiation-hard plastic scintillator for high-luminosity hadron collider." Proc. of Workshop, 1990, Florida State University.